ELSEVIER

Chemical Engineering Journal 139 (2008) 380–389

Chemical Engineering Journal

www.elsevier.com/locate/cej

A novel approach to reduce hydrocarbon emissions from the HCCI engine

Wen Zeng [a,*], Maozhao Xie [b]

[a] School of Aero-Engine and Energy Engineering, Shenyang Institute of Aeronautical Engineering, Shenyang 110034, PR China
[b] School of Energy and Power Engineering, Dalian University of Technology, Dalian 116024, PR China

Received 20 June 2007; received in revised form 8 August 2007; accepted 13 August 2007

Abstract

A novel approach is proposed and investigated to reduce unburned hydrocarbon emissions from a homogeneous charge compression ignition (HCCI) engine by using in-cylinder catalysts. The combustion and emission characteristics of this HCCI engine are numerically simulated in three cases, i.e., the baseline engine with an uncoated piston crown, the engine with a platinum coating on the top and side surfaces of the piston crown (full coated case) and the engine with a platinum coating only on the side surface of the piston crown (partial coated case). A detailed reaction mechanism of methane oxidation on platinum catalyst is adopted. The results show that the unburned hydrocarbons of the HCCI engine arise primarily from sources near the combustion chamber wall, such as flame quenching at the entrance of crevice volumes and at the combustion chamber wall, and the adsorption and desorption of methane into and from the cylinder wall. The in-cylinder catalyst gives rise to a reduction of exhaust unburned hydrocarbon (UHC) emissions by approximately 15% with the full coating of platinum catalyst on the piston crown, however, with the partial coating, the in-cylinder catalyst can reduce the UHC emissions by approximately 20%.

Keywords: Catalytic combustion; HCCI; Hydrocarbon emission; Multidimensional model; Methane

1. Introduction

Because of its high efficiency, very low nitrogen oxide (NO_x) and particulate matter emissions, the homogeneous charge compression ignition (HCCI) engine has recently become the focus of engine research. However, the HCCI engine still fronts some challenges including higher hydrocarbon (HC) and carbon monoxide (CO) emissions, control of ignition timing and limited operating range [1–7]. Furthermore, because of the lower exhaust temperature, dealing with the emissions by the catalytic converter becomes ineffective. Hence, one must find new means to resolve these problems before the HCCI engine can be put into practical applications.

Hydrocarbon emissions arise from HCCI engines because a fraction of the fuel escapes the primary combustion process as a result of incomplete combustion (partial burning and misfiring), flame quenching at the entrance of crevice volumes and at the combustion chamber wall, and the absorption and desorption of fuel vapour into oil layers on the cylinder wall. The crevices between the cylinder wall and the piston being small volumes with narrow entrances are the primary sources of unburned hydrocarbons, and the largest of these crevice volumes is the piston ring pack crevice. All the sources, except partial burning and misfiring, are close to the combustion chamber wall. It is, therefore, likely that the unburned HCs can be reduced at their sources of production by simply using catalytic coatings on the internal cylinder head, piston surface and piston crown. It is worth noting here that the normal surface temperature of the combustion chamber walls is close to the light-off temperature (250–300 °C) for common catalyst materials.

Previous applications of in-cylinder catalysts in spark-ignition engines [8] have demonstrated that the lean limit can be extended with a catalytic coating on the combustion chamber wall. In a more recent study of Dhandapani et al. [9], copper coating on the piston crown led to improved combustion stability and reduced HC emissions. Hu and Ladommatos [10], and Hu [11] reported that unburned HC emissions were reduced by 20% by the deposition of catalytic platinum (Pt)-rhodium (Rh) coatings on the top and side surfaces of the piston in an SI laboratory engine.

* Corresponding author. Tel.: +86 24 89724900.
E-mail address: zengwen927@sohu.com (W. Zeng).

1385-8947/$ – see front matter © 2007 Published by Elsevier B.V.
doi:10.1016/j.cej.2007.08.028

Nomenclature

A	pre-exponential factor
A_s	area of piston surface
c_j	concentration of species j
D_m	Fick's law diffusion coefficient
Ea	activation energy
h_j	specific enthalpy of species j
m	mass
p	fluid pressure
$\dot{s}$	surface reaction rate
S	sticking coefficient
t	time
T	temperature
$\mathbf{u}$	fluid velocity
v	specific volume
v_{st}	Stefan velocity
$\dot{w}$	gas reaction rate
W_j	molecular weight of species j
Y_j	mass fraction of species j
Greek letters	
δ	Diract delta function
$\mathbf{I}$	unit dyadic
λ	second coefficients of viscosity
μ	first coefficients of viscosity
ρ	total mass density
ρ_j	mass density of species j
Subscripts	
j	index of species
T	transpose of matrix

Distinctive from previous studies, a novel method proposed here aims to reduce HC emissions at their sources of production near the combustion chamber walls, and in particular the crevice volume in the top land region of the piston of a HCCI engine. Numerical simulations are carried out to examine the effects of platinum coating of the piston crown on the combustion characteristics and the exhaust HC emissions.

This paper is organized as follows: in the next section, the detailed chemical reaction mechanisms adopted in this work are presented. In Section 3, the schematic piston of the engine used for numerical simulation is shown, and the specifications of this engine are listed. In Section 4, the computational model is shown, and the schematic of KIVA combined with CHEMKIN and DETCHEM soft packages is discussed in detail. In Section 5, through the multidimensional CFD model, the in-cylinder flow field and the inhomogeneity of temperature and species concentration fields are considered, and the effects of in-cylinder catalytic combustion on the ignition timing, the temperature and species concentration fields, and HC, CO and NO_x emissions of the HCCI engine are analyzed. In the last section, conclusions of the paper are given.

2. Chemical kinetic model

2.1. Surface reaction kinetic model

Up to now, detailed surface reaction mechanisms of the hydrocarbon whose carbon atom's number is greater than three have not been built up, and only the detailed surface reaction mechanisms of methane, ethane and ethene on platinum or rhodium surface have been developed. However, as discussed above, detailed chemical kinetics is needed to simulate HCCI combustion. So in this paper, we choose methane as fuel.

As shown in Table 1, the detailed surface reaction mechanism of CH_4 on platinum catalyst consists of 9 gas species, 11 surface species and 26 surface reactions [12]. This reaction mechanism has been verified by results of extensive simulations and experiments [13]. In all simulations of this paper, the surface site density of catalyst coatings is taken as 2.72×10^{-9} mol/cm^2.

2.2. Gas reaction kinetic model

A detailed gas reaction mechanism of methane oxidation is adopted. It consists of 53 species and 325 reactions. This mechanism refers to C/H/O/N chemistry (nitrogen chemistry is included), thus the NO_x emission can be calculated. Through validations by many researchers, good agreements between the simulations and experiments have been obtained [14].

3. Physical model

The engine used for numerical simulation is derived from a Cummins B-series production diesel engine, which is a typical medium-duty diesel engine. This engine was converted into a balanced single-cylinder HCCI research engine through several modifications, as described in Ref. [15]. The engine is equipped with a custom HCCI piston as shown in Fig. 1. In the full-coated case, the top and the side surfaces of the piston crown are coated with catalyst, while in the partial coated case, only the side surface of the piston crown is coated. The sign of the catalyst coating on the side surface of the piston crown is not presented in this figure. The engine specifications and operating conditions are listed in Table 2 [16]. According to the lower ignitibility of methane, in this paper, higher initial temperatures and compression ratio are chosen.

4. Computational model

Because ignition in the HCCI engine occurs at multiple sites simultaneously across the combustion chamber, once the ignition occurs, the gas mixture is consumed quickly even without discernable flame propagation. It is generally accepted that the HCCI combustion is dominated by chemical kinetics and turbulence has little direct effect on HCCI combustion. This would be true if a strictly homogeneous mixture exists during the time of combustion. However, some researchers have reported that the flow field in the cylinder had certain effects on the rates of chemical reactions and the combustion process of HCCI engines

Table 1
Surface reaction mechanism of methane on platinum surface

Reactions	*S*	*A* (mol, cm, s)	Ea (KJ/mol)
$H_2 + Pt(s) + Pt(s) \rightarrow H(s) + H(s)$	0.046E−00		0.0
$H + Pt(s) \rightarrow H(s)$	1.000E−00		0.0
$O_2 + Pt(s) + Pt(s) \rightarrow O(s) + O(s)$	2.300E−02		0.0
$CH_4 + Pt(s) + Pt(s) \rightarrow CH_3(s) + H(s)$	1.000E−02		0.0
$O + Pt(s) \rightarrow O(s)$	1.000E−00		0.0
$H_2O + Pt(s) \rightarrow H_2O(s)$	0.750E+00		0.0
$CO + Pt(s) \rightarrow CO(s)$	8.400E−01		0.0
$OH + Pt(s) \rightarrow OH(s)$	1.000E−00		0.0
$O(s) + H(s) \Leftrightarrow OH(s) + Pt(s)$		3.700E+21	11.5
$H(s) + OH(s)) \Leftrightarrow H_2O(s) + Pt(s)$		3.700E+21	17.4
$OH(s) + OH(s)) \Leftrightarrow H_2O(s) + O(s)$		3.700E+21	48.2
$CO(s) + O(s) \rightarrow CO_2(s) + Pt(s)$		3.700E+21	105.0
$C(s) + O(s) \rightarrow CO(s) + Pt(s)$		3.700E+21	62.8
$CO(s) + Pt(s) \rightarrow C(s) + O(s)$		1.000E+18	184.0
$CH_3(s) + Pt(s) \rightarrow CH_2(s) + H(s)$		3.700E+21	20.0
$CH_2(s) + Pt(s) \rightarrow CH(s) + H(s)$		3.700E+21	20.0
$CH(s) + Pt(s) \rightarrow C(s) + H(s)$		3.700E+21	20.0
$H(s) + H(s) \rightarrow Pt(s) + Pt(s) + H_2$		3.700E+21	67.4
$O(s) + O(s) \rightarrow Pt(s) + Pt(s) + O_2$		3.700E+21	213.0
$H_2O(s) \rightarrow H_2O + Pt(s)$		1.000E+13	40.3
$OH(s) \rightarrow OH + Pt(s)$		1.000E+13	192.8
$CO(s) \rightarrow CO + Pt(s)$		1.000E+13	125.5
$CO_2(s) \rightarrow CO_2 + Pt(s)$		1.000E+13	20.5

[17–19]. This is because there are always small differences in the temperature and concentration inside the cylinder. To take into account this inhomogeneity effect, a multidimensional model is necessary.

In this section, the CHEMKIN chemistry solver [20] and the DETCHEM surface reaction solver [21] are integrated into the KIVA-3V code for solving the chemistry in coupling with multidimensional engine CFD simulations. The KIVA code is used to compute the flow field, including the distributions of mass and temperature in the cylinder, CHEMKIN is used to simulate the gas reactions and DETCHEM is used to simulate the surface reactions.

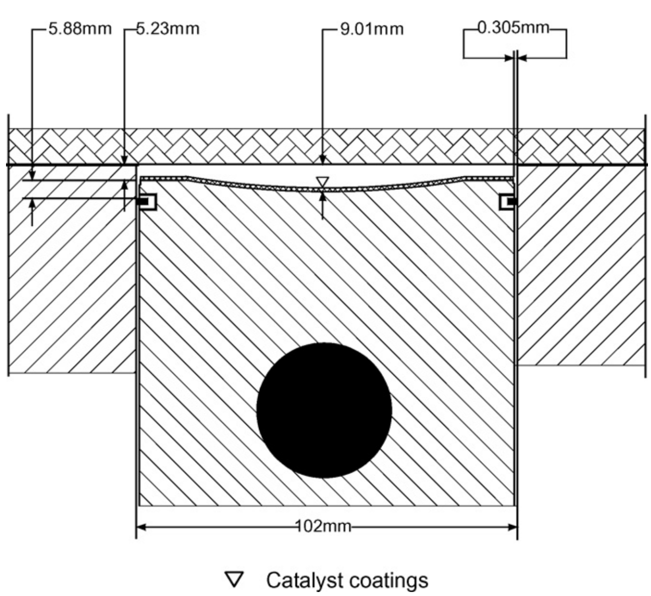

Fig. 1. Schematic of the piston.

The KIVA code solves numerically a set of differential equations governing the in-cylinder processes as follows [22]:

The continuity equation for species *j*:

$$\frac{\partial \rho_j}{\partial t} + \nabla \cdot (\rho_j u) = \nabla \cdot \left[\rho D_m \nabla \left(\frac{\rho_j}{\rho}\right)\right] + \dot{\rho}_j^{c} + \dot{\rho}^{s} \delta_{j1} \quad (1)$$

where, $\dot{\rho}_j^{c}$ and $\dot{\rho}^{s}$ are source terms due to chemistry and the fuel spray. $\dot{\rho}_j^{c}$ can be calculated by

$$\frac{\dot{\rho}_j^{c}}{\rho} = \frac{\mathrm{d}Y_j}{\mathrm{d}t} = vW_j \dot{w}_j + \frac{A_s}{m} \dot{s}_j W_j \quad (2)$$

The boundary condition required at the catalyst-wall is that the gas-phase species mass flux produced by heterogeneous chemical reaction must be balanced by the diffusive flux of that

Table 2
Specifications of the Cummins B-series engine

Bore	102 mm
Compression ratio	17.0
Connecting rod length	192 mm
Engine speed	1200 r/min
EVO	60 BBDC
IVC	25 ABDC
Stroke	120 mm
Intake temperature	470 K
Air excess ratio	3.0
Intake pressure	1.0×10^5 Pa
Wall temperature	400 K
Fuel	Methane

species in the gas:

$$\dot{s}_j W_j = \mathbf{j}_j + \rho Y_j v_{\mathrm{st}} \tag{3}$$

where, the diffusion flux of species **j** is calculated by:

$$\mathbf{j}_j = -D_{m,j}\frac{\partial c_j}{\partial r} \tag{4}$$

The momentum equation for the fluid mixture:

$$\frac{\partial(\rho\mathbf{u})}{\partial t} + \nabla\cdot(\rho\mathbf{uu}) = \frac{1}{\alpha^2}\nabla p - A_0\nabla\left(\frac{2}{3}\rho k\right) + \nabla\cdot\boldsymbol{\sigma} + \mathbf{F}^{\mathrm{s}} + \rho\mathbf{g} \tag{5}$$

where, the dimensionless quantity α is used in conjunction with the Pressure Gradient Scaling (PGS) Method. A_0 is zero in laminar calculations and unity when one of the turbulence models is used. F^{s} is the rate of momentum gain per unit volume due to the spray. The specific body force **g** is assumed constant. The viscous stress tensor σ can be calculated by

$$\boldsymbol{\sigma} = \mu[\nabla\mathbf{u} + (\nabla\mathbf{u})^{\mathrm{T}}] + \lambda\nabla\cdot\mathbf{uI} \tag{6}$$

The internal energy equation:

$$\frac{\partial(\rho I)}{\partial t} + \nabla\cdot(\rho\mathbf{u}I) = -p\nabla\cdot\mathbf{u} + (1 - A_0)\boldsymbol{\sigma} : \nabla\mathbf{u} - \nabla\cdot\mathbf{J} + A_0\rho\varepsilon + \dot{Q}^{\mathrm{c}} + \dot{Q}^{\mathrm{s}} \tag{7}$$

where I is the specific internal energy, exclusive of chemical energy. $\dot{Q}^{\mathrm{c}}$ and $\dot{Q}^{\mathrm{s}}$ are the source terms due to chemical heat release and spray interactions. The heat flux vector **J** is calculated as

$$\mathbf{J} = -K\nabla T - \rho D_m\sum_j h_j\nabla\left(\frac{\rho_j}{\rho}\right) \tag{8}$$

When the $k-\varepsilon$ turbulence model is in use, two additional transport equations are solved for the turbulent kinetic energy k

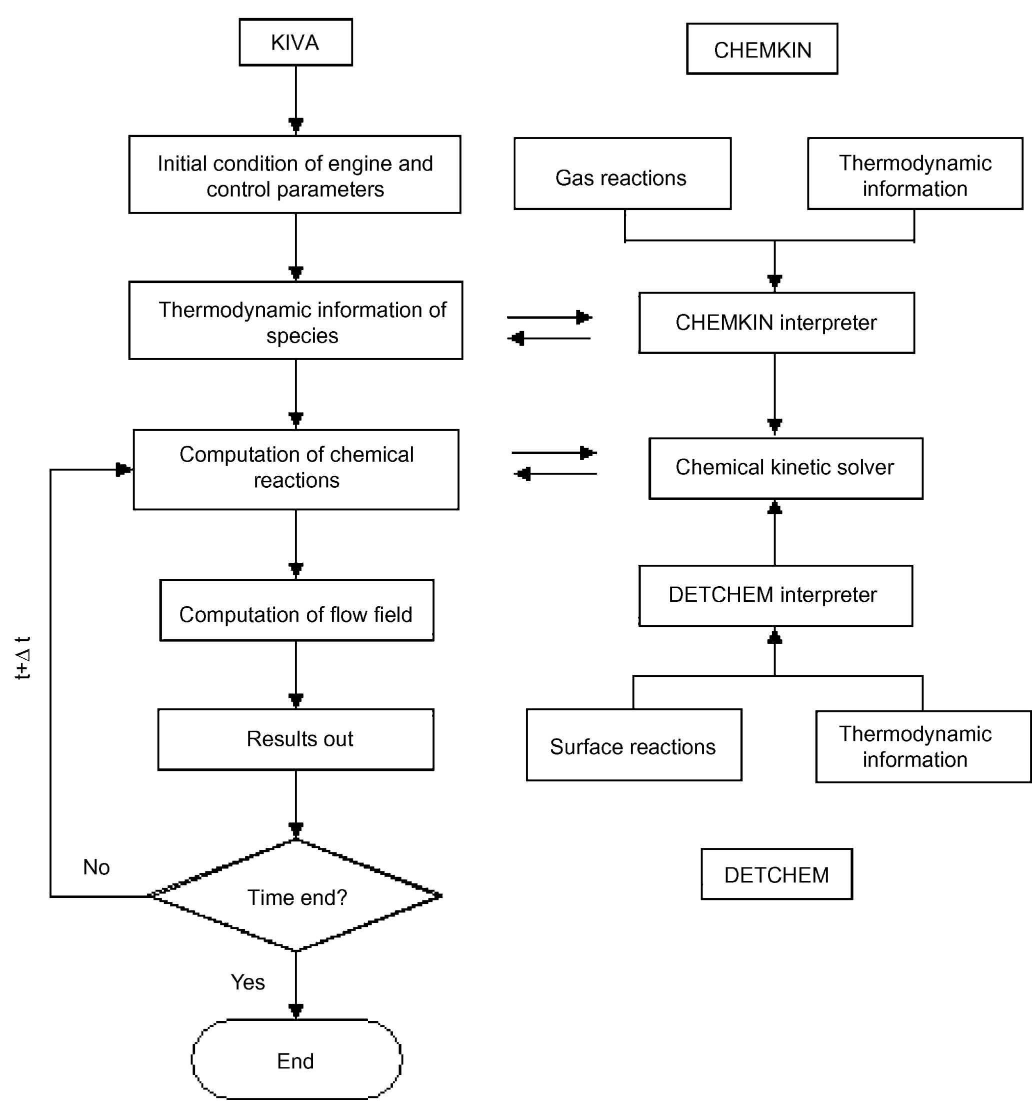

Fig. 2. The combine of KIVA code, CHEMKIN and DETCHEM solvers.

and its dissipation rate ε

$$\frac{\partial(\rho k)}{\partial t} + \nabla\cdot(\rho\mathbf{u}k) = -\frac{2}{3}\rho k\nabla\cdot\mathbf{u} + \boldsymbol{\sigma}:\nabla\mathbf{u} - \nabla\cdot\left[\left(\frac{\mu}{Pr_k}\right)\nabla k\right] - \rho\varepsilon + \dot{W}^{\mathrm{s}} \quad (9)$$

$$\frac{\partial(\rho\varepsilon)}{\partial t} + \nabla\cdot(\rho\mathbf{u}\varepsilon) = -\left(\frac{2}{3}c_{\varepsilon_1} - c_{\varepsilon_1}\right)\rho\varepsilon\nabla\cdot\mathbf{u} + \nabla\cdot\left[\left(\frac{\mu}{Pr_\varepsilon}\right)\nabla\varepsilon\right] + \frac{\varepsilon}{k}(c_{\varepsilon_1}\boldsymbol{\sigma}:\nabla\mathbf{u} - c_{\varepsilon_2}\rho\varepsilon + c_{\mathrm{s}}\dot{W}^{\mathrm{s}}) \quad (10)$$

where $\dot{W}^{\mathrm{s}}$ is a source term due to the fuel spray. $c_{\varepsilon1}$, $c_{\varepsilon2}$, $c_{\varepsilon3}$, Pr_k and Pr_ε are constants whose values are determined from experiments and some theoretical considerations.

To carry out computations, firstly, the interpreters of CHEMKIN and DETCHEM software read the mechanisms of gas and surface reactions, and the thermodynamic information of species. At the same time, these two interpreters translate the thermodynamic information of species from NASA format to JANAF format for KIVA code. In the computing course of flow field and combustion, the KIVA code provides CHEMKIN and DETCHEM with the information of species, temperature and pressure in each computational cell as initial conditions, the CHEMKIN and the DETCHEM solvers then compute the species and heat release in a new time step δt. Afterwards, we return to KIVA to compute the flow field again. The detailed computing flow chart is shown in Fig. 2.

The computation starts from intake valve closure (IVC) to exhaust valve open (EVO), and the distributions of temperature, pressure and species are assumed to be homogenous at the time of intake valve closure. The computing mesh at IVC is shown in Fig. 3. Because platinum catalysts are coated on the piston crown in order to simulate the effects of catalysis on HCCI combustion process, we only need to compute surface reactions in the meshes adjoining the piston crown.

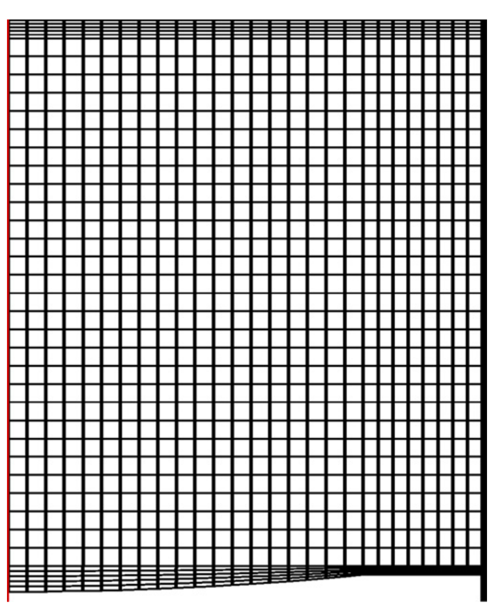

Fig. 3. The computing mesh at 25 ABDC.

5. Computational results

Three engine configurations were simulated: the baseline engine with the uncoated piston crown; engine with full coating on the top and side surfaces of the piston crown and engine with partial coating only on the side surface of the piston crown.

5.1. Effects of in-cylinder catalyst coating on the ignition timing of the HCCI engine

The effects of the catalytic coating on the combustion characteristics are obtained by analyzing the cylinder pressure and the heat release data. The results are shown in Fig. 4.

For clarity, a comparison here is made among the baseline, the partial and the full coatings configurations. The ignition timing is 2 °CA-deg before top dead center (BTDC) for the configurations without as well as with partial coating of catalyst on the piston crown, while it is 3 °CA-deg BTDC in the case of the full coating configuration. The partial coating of catalyst on the side surface of the piston crown has little effect on the primary combustion, thus it leads to nearly the same ignition timing and heat release as the baseline engine. Faster burning rate with the full coating of catalyst on the piston crown is evident from a higher peak in-cylinder pressure and earlier ignition timing. Detailed pressure and heat release analyses of these three configurations show that the main difference in the burning rate exists only during the initial combustion phase. The burning rate or the cylinder pressure in the following stage, during which the majority of the fuel was consumed, is almost unaffected.

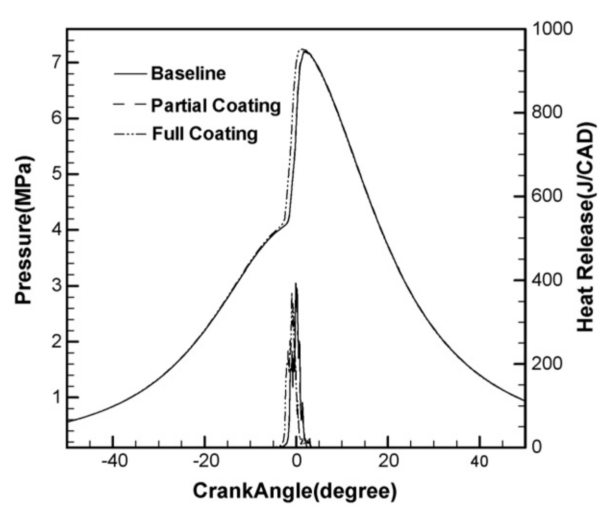

Fig. 4. Comparison of the combustion characteristics of the baseline, partial and full coatings configurations.

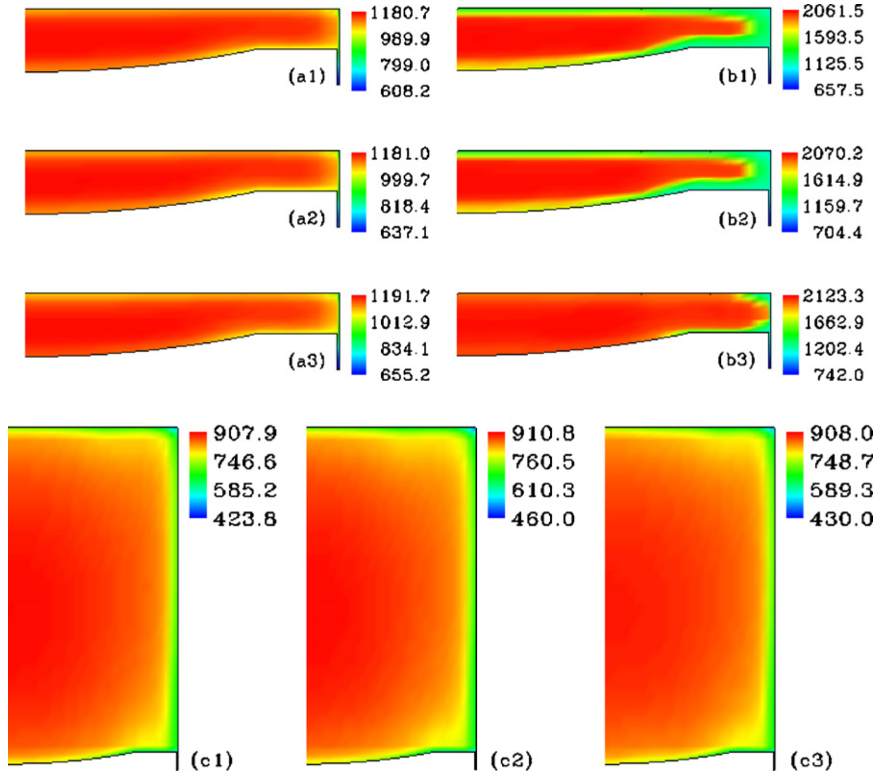

Fig. 5. Comparison of the temperature (K) field in the cylinder of the baseline, partial and full coatings configurations. (a1–a3) The baseline, partial and full coatings of Pt catalyst on the piston crown at 5 °CA-deg BTDC; (b1–b3) The baseline, partial and full coatings of Pt catalyst on the piston crown at 0 °CA-deg BTDC and (c1–3) The baseline, partial and full coatings of Pt catalyst on the piston crown at 120 °CA-deg ATDC.

5.2. Effects of in-cylinder catalyst coating on the temperature field of the HCCI engine

As shown in Fig. 5a, at 5 °CA-deg BTDC, the mixed gas in the whole cylinder cannot be ignited for these three cases of the baseline, the partial and the full coating configurations. However, it should be noted when the piston crown is partial or full coated with Pt catalyst, both the peak temperature of the core region and the lowest temperature in the crevice region are elevated. Especially, in the case of the full coating configuration, compared with the baseline engine, the temperature in the crevice region is elevated by 50 K. At 0 °CA-deg BTDC, as shown in Fig. 5b1 and b2, in the cases of both the baseline and the partial coating configurations, there is a significant temperature gradient in the cylinder, which means that a high temperature region exists in the core region, while in the crevice region and the boundary layer, temperatures are much lower. On the other hand, as shown in Fig. 5b3, when the piston crown is full coated with catalyst, the temperature field in the cylinder becomes essentially homogeneous with considerably elevated temperatures in the boundary layer and the crevice region.

At 120 °CA-deg after top dead center (ATDC), as shown in Fig. 5c, although little difference in the temperature fields can be observed among these three cases, there is still some difference in the peak and the lowest temperatures. Compared with the case of the baseline engine, the lowest temperatures in the crevice regions are higher in the cases of the partial and the full coating configurations. Especially, compared with the case of the full coating configuration, only partial coating has higher temperature in the crevice region.

5.3. Effects of in-cylinder catalyst coating on the HC concentration field of the HCCI engine

The calculated HC concentration fields in the cylinder are presented in Fig. 6. As shown in Fig. 6a1 and a2, at 0 °CA-deg BTDC, for the cases of both the baseline and the partial coating configurations, because of the high temperature in the core region, there the HC concentrations are slight. However, temperatures are low in the regions adjacent to the head and wall of the cylinder as well as to the crevices, the mixtures cannot be oxidized entirely, so there exists a large amount of unburned HC. Contrastively, Fig. 6a3 shows that for the case of full coating configuration, the HC concentration in the whole cylinder is low and distributed homogeneously because of the high temperature and its homogeneity throughout the combustion chamber. However, compared with the partial coating configuration, in the case of full coating, the HC concentration in the crevice region is higher, the reason for that will be discussed later.

At 120 °CA-deg ATDC, as shown in Fig. 6b–c, although the HC concentration fields in the above three cases seem similar, there is still certain difference in the peak and the lowest HC concentrations. Compared with the case of the baseline configuration, both the peak and the lowest HC concentrations are lower

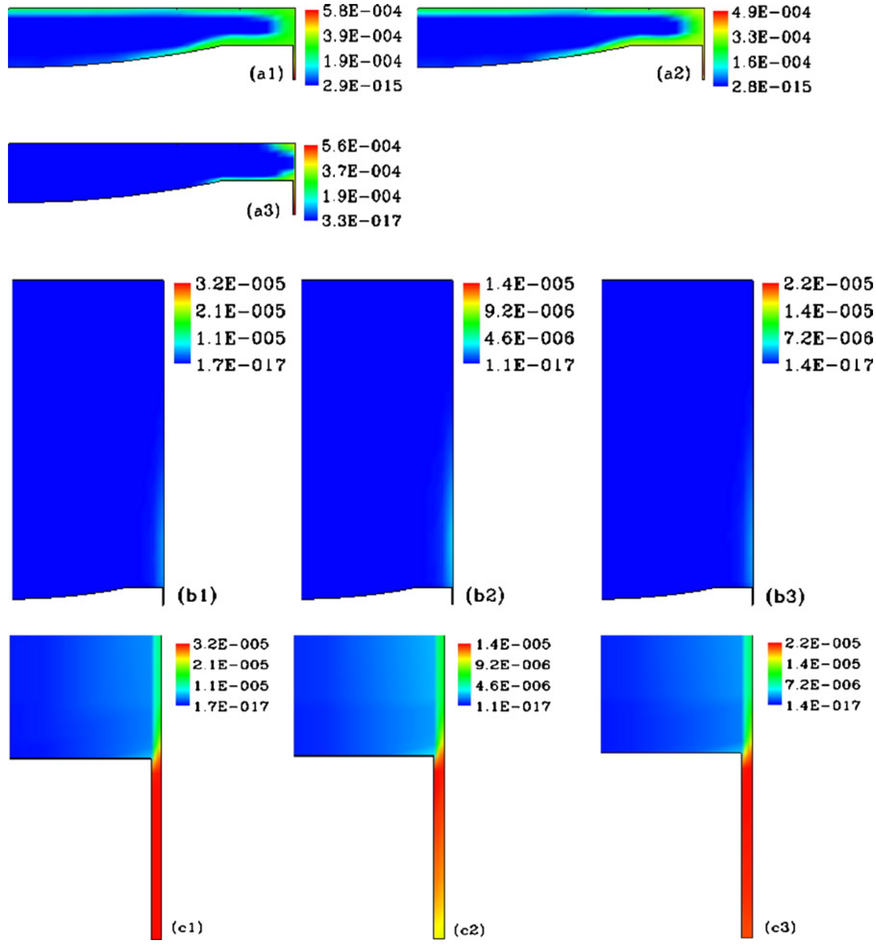

Fig. 6. Comparison of the HC concentration (mass fraction) field in the cylinder of the baseline, partial and full coatings configurations. (a1–a3) The baseline, partial and full coatings of Pt catalyst on the piston crown at 0 °CA-deg BTDC; (b1–b3) The baseline, partial and full coatings of Pt catalyst on the piston crown at 120 °CA-deg ATDC and (c1–c3) Magnified plots of HC distributions in the crevice regions of (b1–b3).

in the case of the full coating configuration. However, the same as at 0 °CA-deg BTDC, compared with the full coating configuration, in the case of partial coating, the HC concentration in the crevice region is lower. It is expected that the catalytic coating on the top surface of the piston resulted in reduced HC emissions, as shown in [23]. It is quite unexpected, however, that the partial coating of the piston crown gives rise to even greater reduction in the exhaust HC emissions than in the case of the full coating configuration. It can be readily explained when the other engine characteristics such as the temperature and the pressure in the cylinder are considered: with catalytic coating on the side surface of the piston crown only, unburned hydrocarbons are reduced by the catalyst coating at their main source of production, i.e., the crevice volume in the top land region of the piston, yet the primary combustion processes are almost unaffected. This explains why the pressure and the heat release are almost the same with the baseline engine. With the same ignition timing, the partial coating on the piston crown results in a higher burned-gas temperature in the crevice region during the exhaust processes than that of the baseline engine and the full coating configuration, and these results in a better post-flame oxidation of unburned hydrocarbons.

5.4. Effects of in-cylinder catalyst coating on the CO concentration field of the HCCI engine

As shown in Fig. 7a1 and a2, at 0 °CA-deg BTDC, in the baseline and the partial coating configurations, the core temperatures are rather high, and most of the mixed gas in the core region is consumed to form CO_2. Because of low temperature in the crevices, the mixed gas cannot be ignited. Consequently, only unburned HC is produced there. Thus, the CO concentrations in these two regions (core and crevice regions) are low. The temperature in the boundary layer is not very high, and CO produced by the oxidation of mixed gas cannot be oxidized further and converted completely to CO_2. Hence, there is a large CO concentration in the boundary layer. Fig. 7a3 shows that, for the case of the full coating configuration, the CO concentration in the whole cylinder is lower and more homogeneous because of the higher temperature level and the homogeneity of temperature field.

At 120 °CA-deg ATDC, as shown in Fig. 7b, although little difference in the CO concentration fields can be observed among the above three cases, there is still some difference in the peak and the lowest CO concentrations. Compared with the baseline

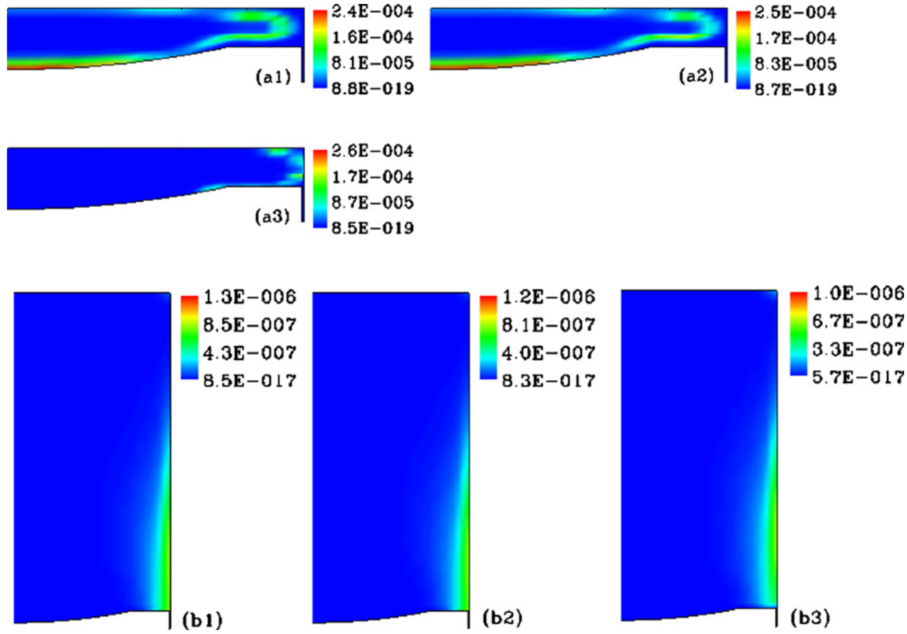

Fig. 7. Comparison of the CO concentration (mass fraction) field in the cylinder of the baseline, partial and full coatings configurations. (a1–3) The baseline, partial and full coatings of Pt catalyst on the piston crown at 0 °CA-deg BTDC and (b1–3) The baseline, partial and full coatings of Pt catalyst on the piston crown at 120 °CA-deg ATDC.

and the partial coating configurations, the peak and the lowest CO concentrations are low in the case of the full coating one.

5.5. *Effects of in-cylinder catalyst coating on the NO concentration field of the HCCI engine*

As shown in Fig. 8a1 and a2, at 0 °CA-deg BTDC, in the case of the baseline and the partial coating configurations, the core temperatures are rather high, but the crevices temperature are lower, and there is a significant temperature gradient in the cylinder. The NO concentration is sensitive to the combustion temperature, so there is also a significant NO concentration gradient in the cylinder. Comparing with the baseline engine, the peak and the lowest NO concentrations are higher in the case of the partial coating configuration. Fig. 8a3 shows that in the case of the full coating configuration, the NO concentration in the whole cylinder is higher than the above two cases because of the higher temperature level.

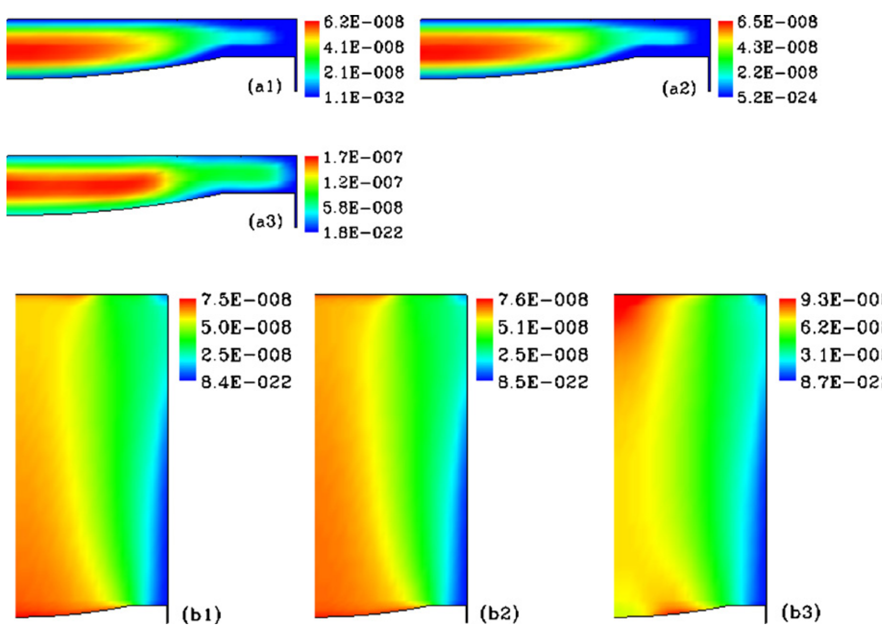

Fig. 8. Comparison of the NO concentration (mass fraction) field in the cylinder of the baseline, partial and full coatings configurations. (a1–3) The baseline, partial and full coatings of Pt catalyst on the piston crown at 0 °CA-deg BTDC and (b1–3) The baseline, partial and full coatings of Pt catalyst on the piston crown at 120 °CA-deg ATDC.

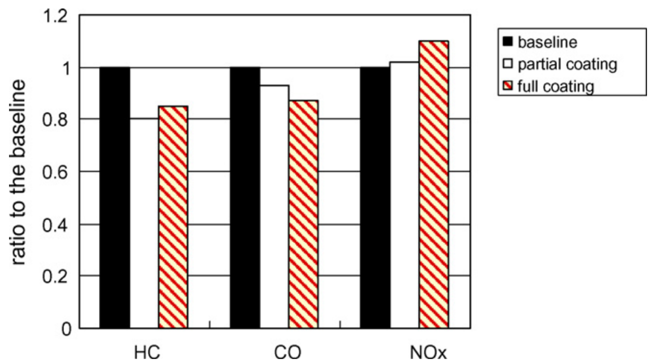

Fig. 9. Comparison of the emissions of the baseline, partial and full coatings configurations.

At 120 °CA-deg ATDC, as shown in Fig. 8b, although little difference in the NO concentration fields can be observed among the above three cases, there is still some difference in the peak and the lowest NO concentrations. Compared with the baseline and the partial coating configurations, the peak and the lowest NO concentrations are higher in the case of the full coating one.

5.6. *Summary of in-cylinder catalyst coating effects on emissions of the HCCI engine*

Fig. 9 presents a general comparison of total emission characteristics among the above three cases: the baseline, the partial coating and the full coating engines. It can be seen that at the same working conditions, compared with the baseline engine, the emissions of HC and CO are decreased by 15% and 13%, respectively in the case of the full coating configuration, while the NO_x emissions is increased roughly by 10%, however, in the case of the partial coating one, the emissions of HC and CO are decreased by 20% and 7%, respectively, while the NO_x emissions is increased only by 2%.

6. Conclusions

In this paper, a novel approach is proposed to reduce unburned hydrocarbon emissions at their sources of production using in-cylinder catalysts on the surfaces of the combustion chamber walls in a HCCI engine. Numerical simulations have been conducted to investigate the effects on the combustion and emission characteristics of the platinum coating on the piston crown. The study produces following results:

(1) Unburned HC emissions are persistently reduced by about 15% with the platinum catalyst full coated on the piston crown. While in the case of the partial coating configuration, unburned HC emissions are reduced even by about 20%.
(2) The exhaust CO emissions are reduced by 13%, but the exhaust NO_x emissions are increased by 10% as a result of the full coating of platinum catalyst on the piston crown. In the case of the partial coating configuration, the exhaust CO emissions are reduced by 7%, while the exhaust NO_x emissions do not change appreciably.
(3) With the platinum catalyst partial coated on the piston crown, the primary combustion processes are almost unaffected and with the same ignition timing. However, the ignition timing of the full coating engine is more advanced than that of the partial coating and baseline engines.

Acknowledgment

This research is supported by the National Key Basic Research Project of China (no. 2001CB209201).

References

[1] R.H. Stanglmaier, C.E. Robert, Homogeneous charge compression ignition (HCCI): benefits, compromises, and future engine applications, SAE Paper 1999-01-3682, 1999.
[2] S.B. Fiveland, D.N. Assanis, Development of a two-zone HCCI combustion model accounting for boundary layer effects, SAE Paper 2001-01-1028, 2001.
[3] S.B. Fiveland, D.N. Assanis, A four-stroke homogeneous charge compression ignition engine simulation for combustion and performance studies, SAE Paper 2000-01-0332, 2000.
[4] S.M. Aceves, D.L. Flowers, C.K. Westbrook, J.R. Smith, W. Pitz, R. Dibble, M. Christensen, B. Johansson, A multi-zone model for prediction of HCCI combustion and emission, SAE Paper 2000-01-0327, 2000.
[5] S.C. Kong, C.D. Marriott, R.D. Reitz, M. Christensen, Modeling and experiments of HCCI engine combustion using detailed chemical kinetics with multidimensional CFD, SAE Paper 2001-01-1026, 2001.
[6] S. Soylu, Examination of combustion characteristics and phasing strategies of a natural gas HCCI engine, Energy Conversion Manage. 46 (2005) 101–119.
[7] M. Christensen, P. Einewall, B. Johansson, Homogeneous charge compression ignition (HCCI) using isooctane, ethanol and natural gas-a comparison with spark-ignition operation, SAE Paper 972874, 1997.
[8] T.J. Rychter, R. Lezanski, S. Wojcicki, Catalytic activation of a charge in a pre-chamber of a SI lean-burn engine. The Combustion Institute. 18th Symposium (int.) on Combustion, 1981, pp. 1815–1824.
[9] S. Dhandapani, B. Nagalingam, K.V. Gopalakrishnan, Some experimental investigations on catalytic combustion of lean burn S.I. engine, in: 25th ISATA Jubilee Int. Symp. on Automotive Technology and Automation, Florence, Italy, 1–5 June, 1992, Paper 920441.
[10] Z.Y. Hu, N. Ladommatos, In-cylinder catalysts-a novel approach to reduce hydrocarbon emissions from spark-ignition engines, SAE Paper 952419, 1995.
[11] Z.Y. Hu, A Mathematical Model for in-cylinder catalytic oxidation of hydrocarbons in spark-ignition engines, SAE Paper 961196, 1996.
[12] O. Deutschmann, <http://detchem.com/mechanisms/>, 2004.
[13] R. Schwiedernoch, S. Tischer, O. Deutschmann, J. Warnatz, Experiment and numerical investigation of the ignition of methane combustion in a platinum-coated honeycomb monolith, in: Proceeding of the Combustion Institute, vol. 29, 2002, pp. 1005–1011.
[14] P. Gregory, D.M.G. Smith, M. Frenklach, W.M. Nigel, B. Eiteneer, M. Goldenberg, C.T. Bowman, R.K. Hanson, S. Song, W.C. Gardiner, V.V. Lissianski, Z.W. Qin, Gri-Mech 3.0, <http://www.me.berkeley.edu/grimech/.2000/>.
[15] J.E. Dec, M. Sjöberg, A parametric study of HCCI combustion—the sources of emissions at low loads and the effects of GDI fuel injection. SAE Paper 2003-01-0752, 2003.
[16] S.M. Aceves, D.L Flowers, F.E. Loza, J.M. Frias, J.E. Dec, M. Sjöberg, R.W. Dibble, R.P. Hessel, Spatial analysis of emissions sources for HCCI combustion at low loads using a multi-zone model, SAE Paper 2004-01-1910, 2004.
[17] S.C. Kong, R.D. Reitz, M. Christensen, B. Johansson, Modeling the effects of geometry generated turbulence on HCCI engine combustion, SAE paper 2003-01-1088, 2003.

[18] S.C. Kong, R.D. Reitz, Use of detailed chemical kinetics to study HCCI engine combustion with consideration of turbulent mixing effects, J. Eng. Gas Turbines Power 124 (2002) 702–707.

[19] S.C. Kong, C.D. Marriott, C.J. Runtland, R.D. Reitz, Experiments and CFD modeling of direct injection gasoline HCCI engine combustion, SAE paper 2002-01-1925, 2002.

[20] R.J. Kee, F.M. Rupley, E. Meeks, J.A. Miller, CHEMKIN-III: a fortran chemical kinetics package for the analysis of gas-phase chemical and plasma kinetics, Sandia National Laboratories Livermore, CA 94551-0969, 1996.

[21] O. Deutschmann, S. Tischer, S. Kleditzsch, C. Correa, D. Chatterjee, J. Warnatz, DETCHEM-Package1.5.4. Steinbeis-Transferzentrum-Simulation Reaktiver Stromungen, Heidelberg, Germany, 2003.

[22] A.A. Amsden, KIVA-3V: a block-structured KIVA program for engines with vertical or canted values, Los Alamos National Laboratory, LA-18818-MS, 1997.

[23] W. Zeng, M.Z. Xie, M. Jia, Numerical investigation on the application of catalytic combustion to HCCI engines, Chem. Eng. J. 127 (2007) 81–93.